Available online at www.sciencedirect.com
ScienceDirect
Journal of Nuclear Materials 374 (2008) 445–452
journal of nuclear materials
www.elsevier.com/locate/jnucmat

Increase in pyrolytic carbon optical anisotropy and density during processing of coated particle fuel due to heat treatment

J.D. Hunn *, G.E. Jellison Jr., R.A. Lowden

Materials Science and Technology Division, Oak Ridge National Laboratory, Oak Ridge, TN 37831-6093, United States

Received 28 August 2007; accepted 26 October 2007

Abstract

Measurements of pyrolytic carbon optical anisotropy and density have been made on a series of tri-isotropic (TRISO) coated particles prepared for the United States Department of Energy's Advanced Gas Reactor Fuel Development and Qualification (AGR) program. These measurements show the effect of varying the deposition conditions, especially the deposition temperature, on the density and optical anisotropy of the carbon layers. Additional heat treatment studies of the coated particles at various stages illustrate the strong effect of post-deposition thermal processing on these two pyrolytic carbon properties. Such post-deposition heat treatment occurs during SiC deposition and fuel compact firing, resulting in increased anisotropy and density of the pyrolytic carbon layers.
Published by Elsevier B.V.

PACS: 28.41.Bm; 28.52.Fa; 42.25.Ja; 81.40.Gh

1. Introduction

The Advanced Gas Reactor Fuel Development and Qualification (AGR) program has been established by the United States Department of Energy (US-DOE) to promote the technology required to produce an approved fuel form for the Very High Temperature Gas Cooled Reactor (VHTR), designated as the premier US-DOE Generation IV near-term reactor concept for the Next Generation Nuclear Plant (NGNP). The proposed fuel type is tri-isotropic (TRISO) coated particle fuel. TRISO fuel consists of spherical fuel kernels (350 or 425 μm diameter low-enriched uranium oxide/uranium carbide for the current AGR program) contained within four concentric layers deposited by fluidized bed chemical vapor deposition. These layers are: a porous carbon layer (buffer), a denser carbon layer (inner pyrolytic carbon or IPyC), a layer of polycrystalline silicon carbide (SiC), and another dense carbon layer (outer pyrolytic carbon or OPyC). The TRISO particles are compacted in a graphite matrix to form the final fuel form, either spheres for a pebble bed or cylinders for a prismatic core (12.5 mm diameter and 25 mm long cylinders for the current AGR program).

In determining the optimal deposition conditions for the pyrolytic carbon layers, it is necessary that several properties of the carbon be considered. These include density, porosity, permeability, and preferred orientation. It has long been understood that structural stability of pyrolytic carbon under irradiation is sensitive to the degree of preferred orientation of the carbon basal planes [1,2]. The preferred orientation in pyrolytic carbon has historically been determined by X-ray diffraction [3–5] or one of several optical techniques [6–10], where the optical anisotropy of the carbon basal planes produces a net macroscopic optical anisotropy in non-isotropic pyrolytic carbon. For measurement on actual TRISO fuel coatings, the sample geometry does not lend itself to X-ray diffraction and optical methods are preferred. Recently, we have developed a new instrument which utilizes generalized ellipsometry to measure the optical anisotropy in pyrolytic carbon with improved resolution and accuracy. This instrument, called the two-modulator generalized ellipsometry microscope or 2-MGEM, uses two polarizer-photoelastic modulator

* Corresponding author. Tel.: +1 865 574 2480; fax: +1 865 574 4186.
E-mail address: hunnjd@ornl.gov (J.D. Hunn).

0022-3115/$ - see front matter Published by Elsevier B.V.
doi:10.1016/j.jnucmat.2007.10.003

pairs, oscillating at two different frequencies in the kilohertz range, to generate and analyze elliptically polarized light. The 2-MGEM can determine the optical polarization properties of the pyrolytic carbon by reflecting the polarized light beam at near normal incidence from a polished cross-section of the coated particle [11–13]. One of these properties, the diattenuation (N), is directly related to the historically measured optical anisotropy factor (OPTAF or OAF), also sometime called optical Bacon anisotropy factor (BAF_O),

$$OAF = R_{max}/R_{min} = 1 + N/1 - N \approx 1 + 2N, \quad (1)$$

where R_{max} (R_{min}) is the maximum (minimum) reflectivity and ideally should occur for light polarized parallel to (perpendicular to) the preferred orientation of the carbon basal planes [14].

Previous transmission electron microscopy (TEM) studies have found that order in pyrolytic carbons often increases as a function of heat treatment or irradiation [15,16]. It is also general knowledge in the TRISO fuel community that heat treatment is expected to increase the optical anisotropy and density of the pyrolytic carbon layers. In this paper, we present results of measurements made with the 2-MGEM, where the high resolution and accuracy of this instrument has enabled a detailed study of the small increases in the optical anisotropy caused by heat treatment of the pyrolytic carbon layers during deposition and subsequent compacting. In addition, we present quantitative analysis of the accompanying increase in the layer density.

2. Experimental

2.1. Processing conditions

TRISO coatings were deposited onto nominally 350 μm diameter low-enrichment uranium oxide/uranium carbide (UCO) kernels by chemical vapor deposition in a 50 mm diameter fluidized bed furnace with a single inlet conical distributor. Table 1 lists the key baseline processing parameters for each layer. Consecutive coatings were applied without removing particles from the coating chamber. Initial average particle surface temperature was determined using an optical pyrometer to observe the top of the fluidized particle bed. During deposition, bed temperature was controlled by maintaining the graphite coating chamber at a constant external temperature. Coating gas fraction (CGF) is the fraction of coating gas in the total gas flow (TGF) used to fluidize the particles. Argon was added to the coating gas to fluidize the particles for the carbon depositions and hydrogen was added to the coating gas for the SiC deposition. Pure argon was used to fluidize the particles and flush the coating chamber between coating steps. After OPyC deposition, particles were allowed to cool to near room temperature under argon fluidization before removal from the furnace. The average deposition rate was calculated from the average coating thickness divided by the deposition time.

In addition to the baseline coating parameters listed in Table 1, four other coating recipes were used to produce TRISO particle lots with slightly modified properties. Each of the five lots was a composite of at least three separate batches produced using the same coating parameters. Table 2 lists the process differences between the baseline and the four variants (changes from baseline are in bold type). Variant 1 was an IPyC process variant where the deposition temperature was increased with the expectation of decreased anisotropy accompanied by a decrease in the density and increase in the permeability. Variant 2 was an IPyC variant designed to increase the deposition rate by increasing the coating gas fraction. Variant 3 was a SiC variant which used a 1:1 mixture of Ar and H for fluidization during SiC deposition to produce a finer grain structure at a lower deposition temperature. Variant 4 used the same coating parameters as the baseline but was carried out as an interrupted process, meaning particles were extracted from the furnace after the IPyC deposition and put into a new coating chamber for deposition of the remaining two layers.

Table 2
Variation in baseline process parameters for five TRISO particle lots

	IPyC temperature (°C)	IPyC coating gas fraction	SiC temperature (°C)
Baseline	1265	0.30	1500
Variant 1	**1290**	0.30	1500
Variant 2	1265	**0.45**	1500
Variant 3[a]	1265	0.30	**1425**
Variant 4[b]	1265	0.30	1500

[a] Variant 3 SiC was deposited using 50:50 mix of Ar:H for the fluidization gas.
[b] Variant 4 was removed from coater between IPyC and SiC depositions.

Table 1
Key baseline process parameters for AGR-1 TRISO particles in this study

	Buffer	IPyC	SiC	OPyC
Deposition temperature	1450 °C	1265 °C	1500 °C	1290 °C
Coating gas ratio	NA	0.85 $\frac{C_3H_6}{C_2H_2}$	NA	0.85 $\frac{C_3H_6}{C_2H_2}$
Coating gas fraction[a]	0.61 $\frac{C_2H_2}{TGF}$	0.30 $\frac{C_2H_2+C_3H_6}{TGF}$	0.012 $\frac{MTS\ in\ H}{TGF}$	0.30 $\frac{C_2H_2+C_3H_6}{TGF}$
Deposition rate[b] (μm/min)	21	3.2	0.25	4.1

[a] TGF = total gas flow, MTS = methyltrichlorosilane (CH_3SiCl_3).
[b] Deposition rate is reported as an average rate over each coating step. The actual deposition rate varies with increasing surface area.

TRISO particles from the first four lots listed in Table 2 (baseline through Variant 3) were fabricated into 12.5 mm diameter, 25 mm long graphite matrix compacts for use in the AGR-1 irradiation test. The particles were over-coated with a mixture of natural and synthetic graphite in a thermosetting resin and then pressed into cylinders. These compacts were heated in helium up to 950 °C to drive off volatiles and carbonize the resin. After 1 h at 950 °C, a final heat treatment of 1 h at 1800 °C in vacuum was performed to drive off any residual impurities and improve thermal conductivity. After the final heat treatment at 1800 °C, some compacts were electrolytically deconsolidated in nitric acid to recover the TRISO particles for further analysis. The Variant 4 TRISO particle lot was not compacted, but some particles from each batch were heated in vacuum for 1 h at 1800 °C using the same furnace ramp rates as were used for compacting to simulate the heat treatment of the particles during compacting.

2.2. Measurement of optical anisotropy

Diattenuation was measured on TRISO coated particle cross-sections using the 2-MGEM. Details on the measurement of diattenuation in coated particle fuel using this instrument can be found in Ref. [13]. Particles were mounted in a thermoplastic epoxy and polished to near midplane using progressively finer diamond compounds on a rotary platen. Each particle cross-section was scanned by the 2-MGEM using an 8 μm diameter analysis spot and a 5 μm raster step size. About 1200 data points were collected for each IPyC layer and about 1500 data points for each OPyC layer. Fig. 1 shows a histogram of the measured local diattenuation values for a typical IPyC layer cross-section in a single baseline particle. Analysis was performed on 10 particles, randomly selected from each lot. The average diattenuation and the standard deviation of the distribution were calculated for each pyrolytic carbon layer in each particle. As an example, Table 3 presents these values for the IPyC layers on 10 particles of baseline TRISO. Table 3 also shows the average error for each measurement, which was determined as described in Ref. [13] by making multiple measurements at each position. The average error gives an estimate of the uncertainty in the measured values. For each particle, the standard deviation in the distribution of the local diattenuation measured at the 1200 different positions is greater than the average error of the measurement at each position. This confirms that the observed variation of the local diattenuation from position to position within a single layer is real, as opposed to only being a statistical fluctuation due to measurement uncertainty. At the bottom of the table, the mean and standard deviation of each data column is given. The standard deviation in the distribution of the average diattenuation of the 10 particles (0.00071) is considerably less than the mean of the standard deviation of the local diattenuation in each individual measurement (0.0023), indicating that the particle to particle variation is much less than the variation of the local diattenuation within a single particle. This was found to be the case for every particle lot discussed in this paper.

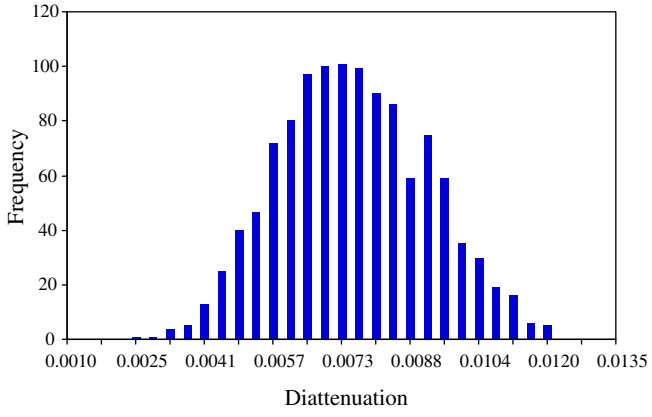

Fig. 1. Example of the distribution in diattenuation observed in the IPyC layer on a single baseline TRISO particle.

Table 3
Results from 2-MGEM analysis of IPyC layer on 10 particles of fully coated baseline

Particle ID	Average diattenuation	Standard deviation	Average error
1	0.0075	0.0017	0.0012
2	0.0066	0.0023	0.0012
3	0.0081	0.0030	0.0012
4	0.0085	0.0023	0.0011
5	0.0069	0.0020	0.0011
6	0.0077	0.0023	0.0014
7	0.0063	0.0025	0.0014
8	0.0080	0.0021	0.0015
9	0.0069	0.0019	0.0014
10	0.0075	0.0024	0.0012
Mean	0.0074	0.0023	0.0013
Standard deviation	0.00071	0.00036	0.00014

The uncertainty in the mean of the average diattenuation can be estimated by the 95% confidence interval for the actual mean of the entire particle lot based on the mean and distribution measured on the random sample of 10 particles from each lot. This was calculated by Eq. (2) using student-t statistics,

$$\bar{x} \pm t\sigma/\sqrt{n}. \tag{2}$$

The interpretation of this interval is that the exact mean value of the lot is undetermined, but to a confidence level of 95%, it is predicted to be within the interval in Eq. (2), where $\bar{x}$ and σ are the measured mean and standard deviation of a random sample of n particles and t is the 95% probability, two-tailed student-t value for $n-1$ degrees of freedom ($t = 2.262$ for $n = 10$). For the example in Table 3, this gives a confidence interval of 0.0069–0.0079. The width of this interval is a product of the particle to particle variation and the number of particles measured, as opposed to stochastic error in the measurement by the 2-MGEM. A similar calculation can be performed to determine the

uncertainty on the average diattenuation for each individual particle. Because of the higher number of data points per particle, this uncertainty is only around ± 0.0001 and does not contribute significantly to the uncertainty in the mean of the average diattenuation for the particle lot.

2.3. Measurement of other physical properties

Results from measurements of coating thickness, density, and open porosity are also reported in this paper. Coating thickness was measured on polished cross-sections using automated imaging and computer analysis. Particles were mounted in a square array using a thermoplastic epoxy and polished to midplane in a similar manner to that used for the anisotropy samples. Imaging on a computer controlled optical microscope was done using an automated routine to capture an image at each position in the square array. The position of the polished plane was determined for each particle and used to correct for imaging the cross-sections slightly off midplane. Each image was processed using custom image analysis software to identify all coating interfaces and measure coating thickness at 360 positions around each layer cross-section [17–19]. The average thickness of each layer in each particle was used to determine a mean thickness and distribution of the layer thicknesses for that particle lot.

The density of the IPyC and OPyC layers was measured using a liquid gradient density column similar to that described in ASTM D1505 [20]. This method determines the sink/float density of a solid, which is somewhere between the ASTM D3766 standard defined skeletal density and envelope density, depending on the degree of penetration of the column liquid into the open porosity of the solid [21]. The liquid gradient density column was constructed using a concentration gradient of tetrachloroethylene and bromoform and covered a density range from 1.8 to 2.0 g/cm^3. Fragments of IPyC and OPyC were mechanically separated by pressing particles between two flat surfaces. IPyC fragments could not be separated once SiC was deposited because of infiltration of SiC into the outer few microns of the IPyC layer. Therefore, IPyC densities on all particle lots except Variant 4 were determined using representative batches removed from the coater before SiC deposition. Three of these representative interrupted batches were generated for each lot using buffer and IPyC coating parameters identical to those used for the TRISO particles in that lot. IPyC density of Variant 4 was measured on a small sample of particles riffled out of each batch when they were extracted from the coater between the IPyC and SiC deposition steps.

Open porosity was measured using a mercury porosimeter. Open porosity was defined as the ratio of the volume of mercury infiltrating through surface pores over the surface area of the sample. The pressure range chosen for this intrusion determination was 1.7–34.5 MPa. This pressure range covered a pore size range from 0.05 to 1 μm and included most of the observed intrusion. Higher pressures were not included due to the onset of compression of the sample. Particles from the representative interrupted batches used for density measurements were also used to measure open porosity of the IPyC layers.

3. Results and discussion

3.1. Key properties of the pyrocarbon layers

Table 4 lists some key physical properties of the IPyC and OPyC layers for the five TRISO particle lots discussed in this paper. Mean values and standard deviations are reported for coating thickness and sink/float density. Coating thickness was measured on ~240 particles randomly selected from each lot and the reported values are the mean and standard deviation of the average coating thickness for all particles in the sample. Density was measured on 40–60

Table 4
Key properties of IPyC and OPyC for five TRISO particle lots

	Coating thickness[a] (μm)	Deposition rate[b] (μm/min)	Sink/Float density[a] (g/cm^3)	Open porosity[c] (mL/m^2)
(a) IPyC				
Baseline	39.4 (2.3)	3.2	1.901 (0.016)	1.19,1.20
Variant 1	40.5 (2.4)	3.4	1.853 (0.014)	1.15, 1.44, 1.47
Variant 2	40.1 (2.8)	5.0	1.912 (0.015)	1.62, 1.66, 1.73
Variant 3	38.8 (2.1)	3.1	–	–
Variant 4	38.8 (2.3)	3.1	1.904 (0.013)	–
(b) OPyC				
Baseline	41.0 (2.1)	4.1	1.907 (0.009)	1.20
Variant 1	41.1 (2.4)	4.1	1.897 (0.015)	1.15
Variant 2	39.8 (2.1)	4.0	1.902 (0.012)	0.92
Variant 3	39.3 (2.1)	3.9	1.913 (0.012)	0.98
Variant 4	39.4 (2.0)	3.9	1.910 (0.008)	0.93

[a] Thickness and density are reported as *mean* (*standard deviation*) for a statistically significant random sample taken from each particle lot. IPyC density was measured on a composite of three representative batches coated with only buffer and IPyC under identical parameters as each TRISO particle lot.
[b] Deposition rate is reported as an average rate over each coating step. The actual deposition rate changes with increasing surface area.
[c] Single measurements of open porosity on different batches are reported. Reported values are volume of Hg intrusion between 1.7 and 34.5 MPa per surface area of sample.

fragments randomly selected from each batch. The results for all the fragments from all the batches in each lot were combined to obtain a mean and standard deviation for that lot. Open porosity is reported in Table 4 for single measurements made on individual coated particle batches and was not measured on every batch. Each open porosity measurement was made on a random sample of 5000–10 000 particles and represents an average value for that coated particle batch.

Table 4 shows that the coating thickness of the pyrolytic carbon layers in all five TRISO particle lots was well controlled and all mean values were less than one standard deviation away from an average thickness of 40 μm. For this reason, coating thickness is not considered to be a contributing factor to any of the observed property variations discussed in this paper.

Buffer and IPyC coating parameters were the same for the baseline, Variant 3, and Variant 4 lots. It can be seen in Table 4 that the deposition rate and density were very consistent for the IPyC layers in these three lots. Variant 1 IPyC had a similar deposition rate but the density was significantly lower for this high temperature variant than for the baseline IPyC. The open porosity of this lower density IPyC tended to be somewhat higher than baseline, although one batch showed an unexplained lower porosity. Variant 2 IPyC was deposited at a significantly higher rate due to the higher reactant concentration. The open porosity was significantly higher than the IPyC in both the baseline and Variant 1 lots, which is expected for a higher deposition rate, based on an earlier parametric study [22]. The slightly higher sink/float density in Variant 2 may be related to the higher open porosity, which might allow greater infiltration of gradient column liquid, effectively reducing the relative displacement volume of the measured fragments compared to the baseline IPyC.

Although the OPyC was deposited using the same coating parameters for all five TRISO particle lots, a slight variation in layer properties can be expected because the OPyC layer deposition is sensitive to variation in the deposition conditions of the previous layers. Each layer deposition also results in a deposition of material on the walls of the coating chamber. This changes the thermal conductivity of the walls which can have some effect on the deposition conditions, especially on the coating temperature. The OPyC layer is also most affected by the cumulative variation in coating thickness of the underlying layers which changes the surface area of the particles in the coater. Table 4 shows a consistent deposition rate for the OPyC in all five TRISO particle lots, but there was a minor variation in the density and open porosity.

3.2. Optical anisotropy of the pyrocarbon layers before and after compacting

Diattenuation of the IPyC and OPyC layers was measured on 10 particles, randomly selected from each of the first four TRISO particle lots listed in Table 2 (baseline through Variant 3). Analysis was performed once for the fully coated particles prior to compacting and once for coated particles deconsolidated from the fuel compacts. Table 5 reports the mean of the average diattenuation of each particle layer and (in parentheses) the mean of the standard deviation in the local diattenuation of each particle, as described in the discussion of Table 3 in the previous section. The mean of the standard deviation illustrates the width of the distribution in the local diattenuation observed on each particle.

Fig. 2 is a graph of the mean of the average diattenuation for each of the first four TRISO particle lots before and after compacting. The error bars span the 95% confidence interval on the actual mean value for the entire particle lot calculated from the mean and standard deviation

Table 5
Diattenuation before and after compacting[a]

	Fully coated particle	After compacting
(a) IPyC		
Baseline	0.0074 (0.0023)	0.0109 (0.0034)
Variant 1	0.0047 (0.0013)	0.0075 (0.0025)
Variant 2	0.0075 (0.0027)	0.0121 (0.0035)
Variant 3	0.0098 (0.0030)	0.0114 (0.0033)
(b) OPyC		
Baseline	0.0063 (0.0023)	0.0111 (0.0034)
Variant 1	0.0044 (0.0018)	0.0102 (0.0034)
Variant 2	0.0059 (0.0028)	0.0097 (0.0036)
Variant 3	0.0071 (0.0029)	0.0120 (0.0040)

[a] Reported values are each based on measurements of 10 particles and reported as the mean of the average diattenuation measured for each particle, with the mean of the standard deviation in the distribution for each particle in parentheses.

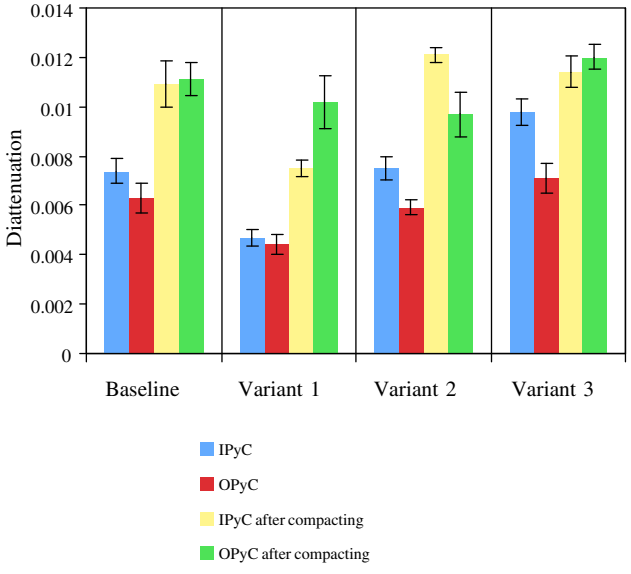

Fig. 2. Mean diattenuation of the pyrolytic carbon layers before and after compacting for first four TRISO particle lots. Error bars show the 95% confidence interval on the mean.

of the 10 measured values of average diattenuation using student-*t* statistics as described in the previous section. From Fig. 2 and Table 5, it can be seen that, in every case, the optical anisotropy of both pyrocarbon layers increased significantly after compacting. This was most probably due to the 1800 °C heat treatment of the particles in the final compacting step. Other factors that could possibly change the diattenuation of the OPyC layer are side effects of the over-coating, low pressure compacting (<60 MPa), and electrolytic deconsolidation processes. However, because of the protective nature of the SiC, none of these processes could reasonably produce a microstructural change in the IPyC layer.

The Variant 1 IPyC layer was found to have significantly lower diattenuation as a result of the 25 °C increase in deposition temperature. This variant also showed an increase in diattenuation after compacting, but it remained significantly lower than all the other pyrolytic carbon diattenuations after compacting. This difference in diattenuation may also be related to the reduced density for this variant. The Variant 2 and baseline particles exhibited very similar IPyC density and diattenuation. Variant 3 appeared to have an anomalously high IPyC diattenuation, given that it was deposited using the same process conditions as the baseline particles. The difference in the SiC deposition conditions between these two lots would not be expected to result in a higher IPyC diattenuation. However, given the broad distribution of the diattenuation within each layer, as indicated by the mean standard deviations in Table 5, there was still significant overlap in the measured values.

As discussed above, the OPyC was deposited using the same coating parameters for all the TRISO particle lots, but some variation in actual deposition conditions can be expected. The OPyC diattenuation before compacting varied some from lot to lot, especially in the case of Variant 1. The lower diattenuation of the Variant 1 OPyC is likely related to the significant difference in the Variant 1 IPyC density and its affect on the thermal conductivity of the coater walls. Variant 1 OPyC also had the lowest observed density (Table 4).

It is difficult to make direct comparison between the IPyC and OPyC layers due to the difference in surface area, fluidization, and coating chamber conditions. For example, the OPyC deposition temperature was 1290 °C (the same as for Variant 1 IPyC). However, given the different coating conditions between IPyC and OPyC, this 25 °C temperature increase was necessary just to reduce the OPyC pyrolytic carbon sink float density to about 1.90 g/cm^3, similar to the baseline IPyC. The OPyC deposition conditions also resulted in a higher deposition rate compared to the baseline IPyC. In the baseline particles, the mean diattenuation of the OPyC layer in the fully coated particles was lower than the IPyC layer diattenuation. This observation is very common in TRISO particle fuel and has been observed by this group of researchers on many batches of particles for many different processing conditions. One key difference between the IPyC and OPyC layers in the fully coated particle is that the IPyC layers are exposed to an elevated temperature during SiC deposition (2 h at 1500 °C for the baseline particles). This added heat treatment is the most likely explanation for the higher diattenuation commonly observed in the IPyC layer. The observation that not only do both baseline pyrolytic carbon layers show increased diattenuation after compacting but also increase to essentially the same value, supports the conclusion that there is a thermally assisted change in microstructure occurring, as opposed to there being a significant difference in the as-deposited microstructure. Furthermore, Variant 3, which was deposited using the same IPyC and OPyC process parameters as baseline, also showed an increase of both pyrolytic carbon layers to the same level after compacting.

3.3. Increase of optical anisotropy with heat treatment

In order to further investigate the effect of temperature on the pyrolytic carbon diattenuation, Variant 4 was analyzed at different stages of processing. Because this variant was fabricated using an interrupted coating process, it was possible to measure the diattenuation of the IPyC layer before and after SiC deposition. Before SiC deposition, the maximum temperature that the IPyC layer experienced

Table 6
Diattenuation at various stages in TRISO fuel processing[a]

	As-deposited	Fully coated particle[b]	After 1800 °C heat treatment[c]
(a) IPyC			
Batch 1	0.0064 (0.0030)	0.0098 (0.0032)	0.0116 (0.0032)
Batch 2	0.0067 (0.0028)	0.0095 (0.0030)	0.0116 (0.0030)
Batch 3	0.0056 (0.0025)	0.0093 (0.0030)	0.0113 (0.0032)
(b) OPyC			
Batch 1	0.0067 (0.0030)	0.0067 (0.0030)	0.0109 (0.0034)
Batch 2	0.0072 (0.0035)	0.0072 (0.0035)	0.0102 (0.0033)
Batch 3	0.0079 (0.0031)	0.0079 (0.0031)	0.0100 (0.0036)

[a] Values are for three coated particle batches from Variant 4 lot. Reported values are each based on measurements of 10 particles and reported as the mean of the average diattenuation measured for each particle, with the mean of the standard deviation in the distribution for each particle in parentheses.
[b] As-deposited IPyC layers receive heat treatment at 1500 °C for 2 h during SiC deposition.
[c] Heat treatment at 1800 °C for 1 h was used to simulate compact firing.

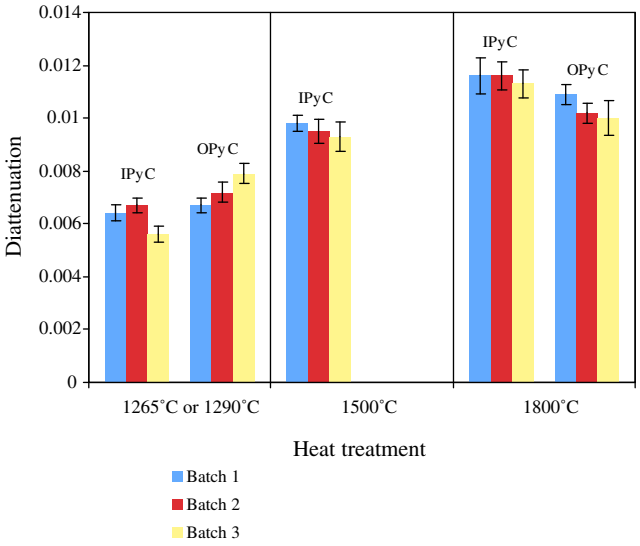

Fig. 3. Mean diattenuation of the pyrolytic carbon layers in Variant 4 at various stages during processing versus maximum heat treatment temperature to which layers were exposed. Error bars show the 95% confidence interval on the mean.

was the IPyC deposition temperature (~1265 °C) which resulted in approximately the same heat treatment that the OPyC layer received in the as-deposited state. In the fully coated TRISO particles, the IPyC received an additional 2 h heat treatment at 1500 °C during SiC deposition, which the OPyC never experienced. To simulate the heat treatment to the particles during compacting, a sample of particles from each batch of Variant 4 was heated in vacuum for 1 h at 1800 °C using the same furnace ramp rates as were used for compacting.

Table 6 reports the results from 2-MGEM measurements on the three coated particle batches in Variant 4, again measuring 10 randomly selected particles for each batch at each condition. The results are reported in terms of the mean and standard deviation, as in Table 5. Fig. 3 shows the measured mean and the 95% confidence interval on the mean of the IPyC and OPyC diattenuations for each batch grouped in terms of the maximum temperature to which the particles were exposed prior to measurement. Prior to deposition of the SiC and coincidental 1500 °C heat treatment, the IPyC diattenuation was essentially equivalent to the OPyC diattenuation. After SiC deposition, the IPyC diattenuation showed a measurable increase. This is the IPyC condition that is usually measured when TRISO fuel is analyzed and explains why the IPyC anisotropy is typically reported to be higher than the OPyC anisotropy. After heat treatment at 1800 °C, both IPyC and OPyC layers showed an additional increase in diattenuation. It is evident, from these results and those on the other TRISO particle lots, that heat treatments at 1500 °C and 1800 °C result in an increase to the optical diattenuation of the pyrolytic carbon layers.

3.4. Increase of density with heat treatment

In order to investigate the effect of heat treatment on the density of the pyrolytic carbon layers, available samples were heat treated and subsequently analyzed in a liquid gradient density column. Table 7 lists the sink/float density of the as-deposited layers, the IPyC layers after 2 h heat treatment at 1500 °C (to simulate SiC deposition), and the IPyC and OPyC layers after 1 h heat treatment at 1800 °C (to simulate compact firing). The density of both pyrolytic carbon layers increased as a result of each heat treatment. Fig. 4 plots the sink/float density versus the diattenuation of all the measured OPyC layers. In this figure, a correlation between the heat treatment effect on density and diattenuation is apparent. All the OPyC layers analyzed in this study were deposited under essentially identical conditions (although slight variation in properties resulted from the effect of changing underlying coating conditions, as discussed earlier). Fig. 4 suggests that the minor variations in the density and diattenuation of the OPyC layers (probably due to a slight variation in

Table 7
Sink/float density at various stages in TRISO fuel processing[a]

	As-deposited	After 1500 °C heat treatment[b]	After 1800 °C heat treatment[c]
(a) IPyC			
Baseline	1.901 (0.016)	1.927 (0.018)	1.953 (0.017)
Variant 1	1.853 (0.014)	1.869 (0.014)	1.892 (0.014)
Variant 2	1.912 (0.015)	1.942 (0.022)	1.968 (0.015)
Variant 3	–	–	–
Variant 4	1.904 (0.013)	–	–
(b) OPyC			
Baseline	1.907 (0.009)	–	1.940 (0.008)
Variant 1	1.897 (0.015)	–	1.922 (0.016)
Variant 2	1.902 (0.012)	–	1.922 (0.013)
Variant 3	1.913 (0.012)	–	1.937 (0.016)
Variant 4	1.910 (0.008)	–	1.937 (0.008)

[a] Density is reported as *mean* (*standard deviation*) for a statistically significant random sample taken from each particle lot. IPyC density was measured on a composite of three representative batches coated with only buffer and IPyC under identical parameters as each TRISO particle lot.
[b] Heat treatment at 1500 °C for 2 h was used to simulate heat treatment of IPyC in fully coated particle.
[c] Heat treatment at 1800 °C for 1 h was used to simulate compact firing.

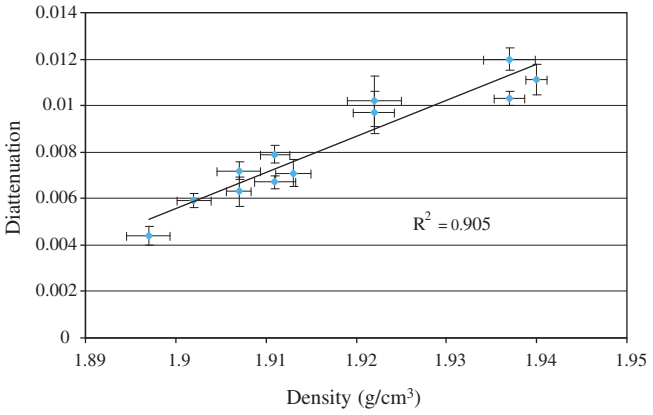

Fig. 4. Mean diattenuation versus mean sink/float density for OPyC layers from each AGR-1 variant, before and after annealing for 1 h at 1800 °C. Error bars show the 95% confidence interval on the mean.

deposition temperature) and the major variations due to post-deposition heat treatment are probably related to the same thermally induced microstructure changes. Analysis of the IPyC layers, which were not deposited under similar conditions, did not show as strong a linear correlation, although the trend for the higher density layers to exhibit a higher diattenuation was still present. In these layers, larger variations in the deposition conditions apparently produced more significant changes in the as-deposited microstructure.

4. Conclusion

The density and diattenuation of the pyrolytic carbon layers was measured on several TRISO particle variants prepared for irradiation testing under the US-DOE Advanced Gas Reactor Fuel Development and Qualification program. A study of these results showed that, not only can these properties be affected by deposition conditions, but also a measurable (and probably related) increase in the anisotropy and density occurs as a result of heat treatment of the particles during coating and compacting. It was also noted that the higher anisotropy usually observed in the inner pyrolytic carbon layer in fully coated TRISO particles, compared to a similarly deposited outer pyrolytic carbon layer, is most likely due to heat treatment of the inner layer during SiC deposition, and that this difference can go away after higher temperature heat treatment during compacting. Because of the observed increase in density and diattenuation after compacting, measurement of these properties after final fabrication of the fuel compacts may be important for predicting fuel performance and for fuel acceptance testing, as opposed to the current general practice of measuring pyrolytic carbon anisotropy on TRISO particles before compacting and sink/float density on as-deposited carbon layers.

Acknowledgements

Research was sponsored by the US-DOE Office of Nuclear Energy, Science and Technology's Advanced Gas Reactor Fuel Development and Qualification program and by the Oak Ridge National Laboratory, managed by UT-Battelle, LLC for the US Department of Energy under Contract No. DE-ACO5-00OR22725.

References

[1] J.C. Bokros, R.J. Price, Carbon 4 (1966) 441.
[2] J.C. Bokros, R.J. Price, Carbon 5 (1967) 301.
[3] G.E. Bacon, J. Appl. Chem. 6 (1956) 477.
[4] J.C. Bokros, Carbon 3 (1965) 167.
[5] P.A. Tempest, Carbon 16 (1978) 171.
[6] R.J. Gray, J.V. Cathcart, J. Nucl. Mater. 19 (1966) 81.
[7] O.M. Stansfield, J. Nucl. Mater. 34 (1970) 215.
[8] V.J. Tennery, C.S. Yust, P. Krautwasser, R.L. Beatty, J. Am. Ceram. Soc. 60 (1977) 268.
[9] A. Inspektor, Y. Hornik, U. Carmi, R. Avni, E. Wallura, H. Hoven, K. Koizlik, H. Nickel, Thin Solid Films 72 (1980) 195.
[10] D.W. Stevens, Surface Science 96 (1980) 174.
[11] G.E. Jellison Jr., J.D. Hunn, R.A. Lowden, J. Nucl. Mater. 352 (2006) 6.
[12] G.E. Jellison Jr., J.D. Hunn, C.M. Rouleau, Appl. Opt. 45 (2006) 5479.
[13] G.E. Jellison Jr., J.D. Hunn, J. Nucl. Mater (2007), doi:10.1016/j.jnucmat.2007.02.008.
[14] K. Koizlik, Carbon 11 (1975) 677.
[15] P. Krautwasser, H. Nickel, C.S. Yust, Carbon 14 (1976) 307.
[16] E. Pollman, J. Pelissier, C.S. Yust, J.L. Kaye, Nucl. Tech. 35 (1977) 301.
[17] J.R. Price, D. Aykac, J.D. Hunn, A.K. Kercher, in: Proceedings of Machine Vision Applications in Industrial Inspection XV, SPIE vol. 6503, 2007.
[18] J.R. Price, D.B. Aykac, J.D. Hunn, A.K. Kercher, R.N. Morris, in: Proceedings of Machine Vision Applications in Industrial Inspection XIV, SPIE vol. 6070, 2006, p. 153.
[19] J.R. Price, J.D. Hunn, in: Proceedings of Machine Vision Applications in Industrial Inspection XII, SPIE vol. 5303, 2004, p. 137.
[20] ASTM D1505-98, ASTM International, West Conshohocken, PA, 1999.
[21] ASTM D3766-86, ASTM International, West Conshohocken, PA, 2003.
[22] R.A. Lowden, J.D. Hunn, S.D. Nunn, A.K. Kercher, J.R. Price, P.A. Menchhofer, G.E. Jellison Jr., ORNL internal report, ORNL/TM-2005/533.